Journal of Metals, Materials and Minerals, Vol. 30, No. 4, pp. 60-67, 2020

Soldering of copper using graphene-phosphoric acid gel

Gurudatt PURANIK[1,2], Asis SARKAR[3], Nirankar MISHRA[3], Sangam Chandrasekhar GURUMURTHY[4] and Shridhar MUNDINAMANI[1,*]

[1] *Device Lab, Department of Physics, Siddaganga Institute of Technology, Tumakuru, Karnataka, 572103, India*
[2] *Department of Mechanical Engineering, Siddaganga Institute of Technology, Tumakuru, Karnataka, 572103, India*
[3] *Department of Nanotechnology, Siddaganga Institute of Technology, Tumakuru, Karnataka, 572103, India*
[4] *Nanomaterials and Polymer Physics Lab, Department of Physics, Manipal Institute of Technology, Manipal Academy of Higher Education, Manipal, Karnataka, 576104, India*

***Corresponding author e-mail:** mpshridhar@sit.ac.in

Received date:
4 January 2020
Revised date
7 August 2020
Accepted date:
9 August 2020

Keywords:
Soldering flux;
Carbon nanomaterials;
Graphene

Abstract

Soldering is a physical process in which one metal melts and joins the other to form a strong bond, which further helps in electron conduction and increases the mechanical strength in any electronic circuits. The present work demonstrates the development of graphene-based flux comprising of 2 g of graphene and 2 ml of phosphoric acid for the residue-free, high stability, durable, and two-step soldering of copper wire on to the surface of the copper-based printed circuit board. The soldering flux can be applied to the copper, and wire can be soldered in ambient conditions using commercial soldering iron at a standard soldering temperature of 260°C. This flux helps the formation of strong and electrically conducting joints between the copper wire and copper-based printed circuit board. The joints are studied with scanning electron microscope images, and energy dispersive X-ray mapping successfully shows the formation of a joint between the copper wire and the copper and also shows the presence of graphene between the joint.

1. Introduction

Solder joints play a vital role in packaging of electronic devices, provides better electrical conductivity and mechanical properties between active electronic components and the substrates. Reliability of solder joints is the key factor which affects electronic products in the long-term usage [1]. Solder is a material used for the interconnection in electronic circuits. Solder materials are becoming the crucial element in an electronic industry due to the concerns related to environment and health which are caused by the electronic waste [2]. Currently there are several promising solder materials such as Sn-Pb, Sn-Au, Sn-In, Sn-Ag, Sn-Zn, Sn-Bi and Sn-Ag-Cu [2]. In addition, these alloys exhibit important parameters like lower melting point and better mechanical properties and lack of hazardous whiskers in the solder joint. Soldering process in electronic industry always results in formation of intermetallic phases. These intermetallic phases are brittle and reduce the mechanical strength and electrical properties of the solder joint. Rapid growth of intermetallic compound layer between solder and the substrate affects the properties of solder joints. Hence it is necessary to control the growth kinetics of these intermetallic compound layers. New technologies and materials are developed by the researchers to avoid the formation of intermetallic compounds [3]. TiO_2 nanoparticles were added to solder to reduce the thickness of the intermetallic compound layers [4]. Graphene is a two-dimensional material consisting of a layer of carbon atoms with sp^2 hybridization arranged in a honeycomb lattice [5]. Its properties include high strength and good electrical and thermal conductivity. The stacked form of graphene is graphite [6]. Graphene has remarkable physical and chemical properties, which makes it a sought-after material for applications in various fields like electronics, biomedicine, energy, and environment [7]. It is the thinnest material, which is one atomic layer thick. Graphene has the same carbon structure as the graphite and is incredibly flexible [8]. Its charge carrier's exhibit giant intrinsic mobility, have zero effective mass, and can travel for micrometres without scattering at room temperature [9]. Graphene can sustain current densities six orders of magnitude higher than that of copper, shows record thermal conductivity and stiffness [9]. The most significant characteristic of graphene is its specific surface area which is upto 2675 $m^2 \cdot g^{-1}$ [10]. Another attractive property of the graphene is, it expands when cooled and shrinks when it is heated [11].

Presently, graphene is very well dominating in fields like electrical, electronics, mechanical, medical innovations, and defence [12]. Graphene or reduced graphene oxide flakes are used for composite materials, conductive paints, and planar graphene is used for high-performance electronic devices. Graphene is a new material that may help researchers in many useful ways, and it can be readily chemically functionalized [13]. Graphene coatings have several applications in electronics, like it can act as a corrosion protection layer and prevents electromigration, during the soldering process it can act as a barrier for the formation of intermetallic compound layers which forms between solder and the substrates [3]. There are no reports, where graphene is used as a flux material in the soldering

process of electrical connections. For the first time, we report the use of graphene as a soldering flux to make better electrical connections.

In soldering electrical connections, the primary difficulty to be overcome is the removal of an oxide layer which forms on the surface of the metal. The oxide film must be removed either chemically or mechanically to establish contact between the solder and metal. Therefore, a flux used as a chemical in the soldering process, which helps to diffuse the free elements to form a joint. Flux permits the solder to adhere to the clean metal surface rather than creating beads, as it would, on an oxidized surface. The most commonly used fluxing agents are rosin flux and chlorides. The present work reports the development of graphene-based flux, which helps to achieve better contact and prevents the damage of the surface by an oxide layer, and graphene enhances the ionic diffusion. Since the developed flux is based on graphene, graphene can be produced on a large scale with a low cost, and the flux can be used in commercial electronic industrial applications.

2. Experimental

All the chemicals and reagents are used as received without any further purification. Carbon powder (graphite), sulphuric acid (H_2SO_4), acetone $(CH_3)_2CO$, isopropyl alcohol (IPA) (C_3H_8O) and potassium permanganate ($KMnO_4$) are obtained from HIMEDIA, India, and ortho-phosphoric acid (OPA) (H_3PO_4) is procured from Thermo Fisher Scientific India Pvt Ltd, India. For all the reactions and cleaning, milli-Q water (specific resistance, 18.2 MΩ·cm) is used. Commercially available printed circuit board (PCB) of copper (Cu) is used and cut into required dimensions of $1 \times 1 \times 0.2$ cm. These pieces are cleaned to remove the dirt by sonicating in acetone, IPA, and milli-Q water for 15 min and are dried in room conditions. Commercially available Aadway BIC solder wire made with Tin/Lead raw material (22 Swg, Red Deluxe) is procured from the local market. Melting temperature of solder wire is 210°C and soldering temperature is 260°C.

The graphene/graphene oxide is synthesized by various methods like Hummer's method [14], chemical vapour deposition [15], chemical exfoliation [16], and electrochemical exfoliation [17]. The properties of graphene mainly depend on the quality of raw material, type of defects, and impurities. In the present work, graphene oxide is synthesized by Hummer's method [14]. Initially, 2 g of graphite powder is added to the round bottom conical flask, and 64.8 ml of H_2SO_4 is added slowly, and the solution is stirred for 30 min, then 9 g of $KMnO_4$ is added slowly to the slurry of graphite powder, which is kept in ice bath to control the heat produced by the exothermic reaction [18]. The colloidal solution of graphene oxide (GO) is centrifuged and washed rigorously with distilled water to achieve a neutral pH. Graphene sheets are prepared by a doctor blade method using the collected slurry of graphene oxide. The resulting sheets are then reduced thermally at 500°C and blended in a mortar and pestle for 30 min and it is used as a starting material in the development of soldering flux. Blended reduced graphene sheets are multi-layered graphene, here-after this multi-layered graphene is referred as graphene.

The soldering composition consists of 2 g of graphene mixed with 2 ml of ortho-phosphoric acid (OPA). The mixture is ground continuously for a three-hour duration in a mortar and pestle. The mixture is blended well until the perfect association between the two is obtained. The obtained composite is used as the intermediate agent to initiate the soldering process. After the soldering process, the sample is washed with IPA to remove the extra OPA. The result of the soldering process is studied by scanning electron microscope (SEM) using the instrument FE-SEM Ultra 55 microscope, Carl Zeiss, Germany, with the acceleration voltage between 2 and 10 kV as found with electron diffraction spectroscopy (EDS). It involves the interaction of an electron beam with a sample target that produces X-rays. An energy-dispersive (EDS) detector is used to separate the characteristic X-rays of different elements into an energy spectrum, and the EDS system is used to analyse the energy spectrum to determine the abundance of specific elements. The crystal structure understood by X-ray diffractometer, Bruker D8 Advance with wavelength 1.54046 Å. The Raman measurements performed on Horiba Jobin Yvon, XploRA PLUS V1.2 Multiline. The mass of graphene measured by Shimadzu AX200 microbalance. Current-voltage characteristics are carried out using Keithley 2450 EC workstation programmed with LabView 2019.

3. Results and discussion

The scanning electron microscope images of the substrate and Cu wire using the graphene-based flux and solder are shown in Figure 1(a-d). Figure 1(a) is the backscattered electron detector (BED) image of Cu wire soldered on the PCB. The shiny upper part of the image shows solder, and the black rod-like structure is a soldered Cu wire. Black tiny dots surrounding the solder are of soldering flux that gets scattered due to the introduction of the high-temperature tip of soldering gun during the soldering process. The secondary electron detector (SED) image shown in Figure 1(b) signifies the interface between Cu, solder, and Cu wire. It confirms the adequate bonding between the three. Figure 1(c) shows SED image of graphene. It clearly shows that the graphene is trapped between the solder and Cu and helps in superior conduction of electrons through the interface with less resistance. Excess graphene has emerged out of the interface during the soldering process. It also shows the graphene crystallites, which are distributed randomly with different orientations. Figure 1(d) is magnified SED image of Figure 1(c) that shows two-dimensional graphene flakes with crystallite size ranging from 0.5 to 4 μm. The conductivity of graphene is inversely proportional to the thickness of graphene sheets [19].

X-ray diffraction is carried out to understand the structure of synthesized graphene, and is shown in Figure 2. A small characteristic peak of (001) plane at 14° and a broad peak of (002) plane at 24° observed. The broadening and shift of the characteristic diffraction peak are due to the short-range order in stacked graphene layers. The observed interlayer spacing of graphene is 3.7Å, and it is slightly larger than that of standard graphite, which results from the small amount of residual oxygen-containing functional groups or other such structural defects present in the material [20].

The prepared GO and graphene are characterized by Raman spectra, which allow the consideration of the conjugated and carbon-carbon double bonds, which lead to high-intensity peaks in the Raman spectrum, as shown in Figure 3. The Raman spectrum of GO is analysed by the G band (graphite lattice) at wavenumber 1592 cm^{-1}, which corresponds to E_{2g} phonon of the sp^2 C atoms, and the D band (disorder band) caused by the graphitic edges at 1338 cm^{-1} corresponds to the k-point phonons of A_{1g} symmetry. The G band of graphene

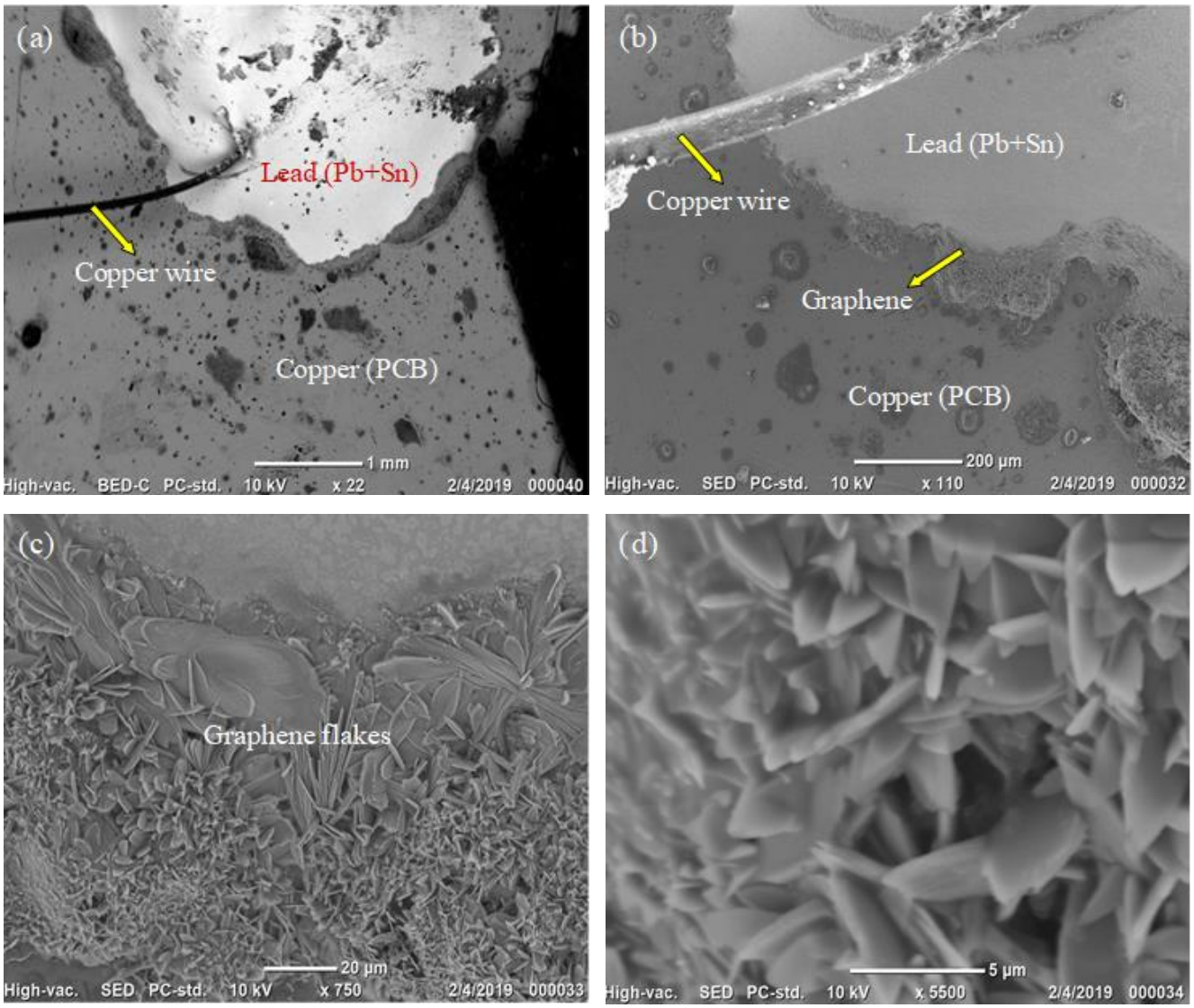

Figure 1. Scanning electron microscopic images of (a) backscattered electron detector image of PCB, soldered copper wire, (b) Secondary electron detector image of PCB, soldered copper wire, (c) Magnification of Secondary electron detector image of PCB, soldered copper wire and (d) Higher magnification of Secondary electron detector image of PCB, soldered copper wire.

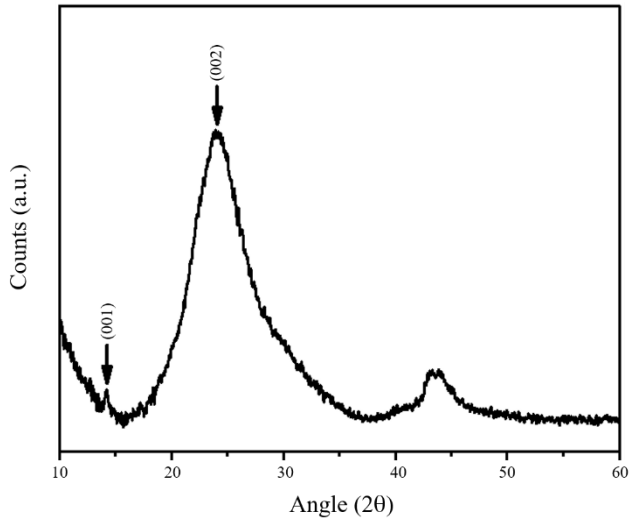

Figure 2. X-ray diffraction pattern of graphene.

observed at 1582 cm^{-1}, and it is shifted slightly from the position of GO, as shown in the inset of Figure 3. The disorder band D band arises from defects like grain boundaries, amorphous carbon species, and vacancies. The I_d/I_g ratio of D and G bands indicate the quality of the product [21]. The band intensity ratio is 0.89 in case of graphene and for GO the ratio is 0.88. The difference 0.01 indicates the synthesized GO and graphene are having large number of structural defects showing the alteration of GO structure through thermal reduction process [22]. It confirms the prepared GO and graphene contain defects, as reported in the literature [23]. The two other bands observed at 2700 and 2900 cm^{-1}. For monolayer graphene, sharp peak at 2700 cm^{-1} is observed [24]. The band at 2700 cm^{-1} is known as 2D band, which indicates the number of layers. The observed broadened 2D band at 2700 cm^{-1} signifies the multi-layered graphene with defects.

Energy dispersive spectroscopic (EDS) analysis is carried out for the area marked with a yellow square line that shows the interface of the bonding area, as shown in Figure 4(a). The EDS analysis graph is represented as Figure 4(b), and it shows the elemental percentage

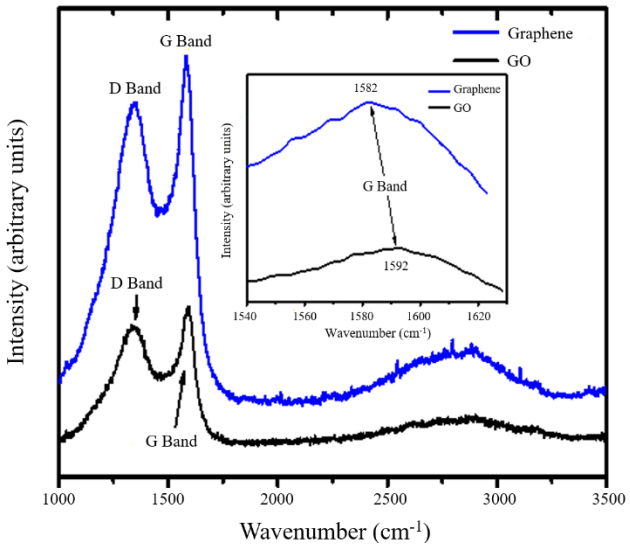

Figure 3. Raman spectrum of graphene oxide and graphene and the inset shows the G band of graphene oxide and graphene.

present in the marked area. EDS analysis in SEM mainly depends on the size of the interaction volume and controlled by the accelerating voltage and the mean atomic number of the elements [25]. All the elements used as precursors in soldering process observed as shown in Figure 4(b). Mainly concentration of copper from the PCB is found to be highest with 34.46% and carbon (graphene) is at 6.34%. The presence of oxygen with 15.90% is due to the oxidation of copper which is open to atmosphere. Table S1 shows the wt% of different elements and also gives concentration in terms of the mass fraction. The atomic (molar) ratios of the elements are related to the wt% through the atomic masses of the elements. The table headers show elements in the first column, series-characteristic X-ray lines in the second column, unn. C [wt%]-unnormalized concentration in wt% of the elements in third column, Norm. C [wt%]- normalized concentration in wt% of the elements in fourth column, Atom. C [at%]- atomic wt% in fifth column and error [wt%]- error in the wt% concentration at one sigma level, as shown in column six. The percentage of Cu, lead, and tin are high when compared with the percentage of other present elements as mentioned in Table S1 (first sample) and Table S2 (fifth sample). The tin and lead are with wt% of 28.59 and 20.19, respectively, from the solder, which is used in the soldering process. Since copper does not wet graphene, there is no diffusion of graphene into copper at the working temperature. Present work started with 6.5±0.3 wt% of graphene and by EDS it is confirmed that the presence of graphene is 6.34±0.2 wt%. EDS mapping is carried out for five different samples and the wt% of graphene is varied from 6.2±0.3 wt% to 6.78±0.3 wt%. Therefore, wt% of graphene left in the solder joint is almost 100%.

The magnified SED image of the interface of Cu, graphene, and solder shows the graphene flakes sandwiched between Cu and solder, as marked in Figure 5(a), which in turn results in the better electrical conduction. The flakes are observed due to its 2-D crystalline lattice, which further helps in the diffusion with less resistance. Graphene with good thermal conductivity tends to combine with molten solder that helps to adhere solder with the oxidized surface of Cu on the PCB. The crystallite size of graphene at the interface is minimal compared to the surrounding graphene as shown in the left bottom corner of Figure 5(a). The magnified BED image of the interface of Cu and solder showed in Figure 5(b). Shiny silver color in the top right corner is of solder, and the greyish color in the left bottom corner is of surrounding graphene, which scatters on the excess Cu of PCB during the soldering process. The diagonal black line in the top right corner indicates the sandwiched graphene between the solder and the copper.

The elemental mapping is carried out to understand the interfaces between Cu, solder, and graphene, and shown in Figure 6(a-e). In which Figure 6(a) shows the standard SEM image where the elemental analysis is carried out. Graphene is the vital material in the present work for the soldering process, carbon mapping is characterized and shown as red color in Figure 6(b), and the remaining black color is the part of Cu and solder. As graphene possesses high mechanical strength and stiffness, it does not flow over the substrate and hence provides excellent stability during the process. The composition of the solder includes tin and lead; thus, the mapping for these elements are carried out

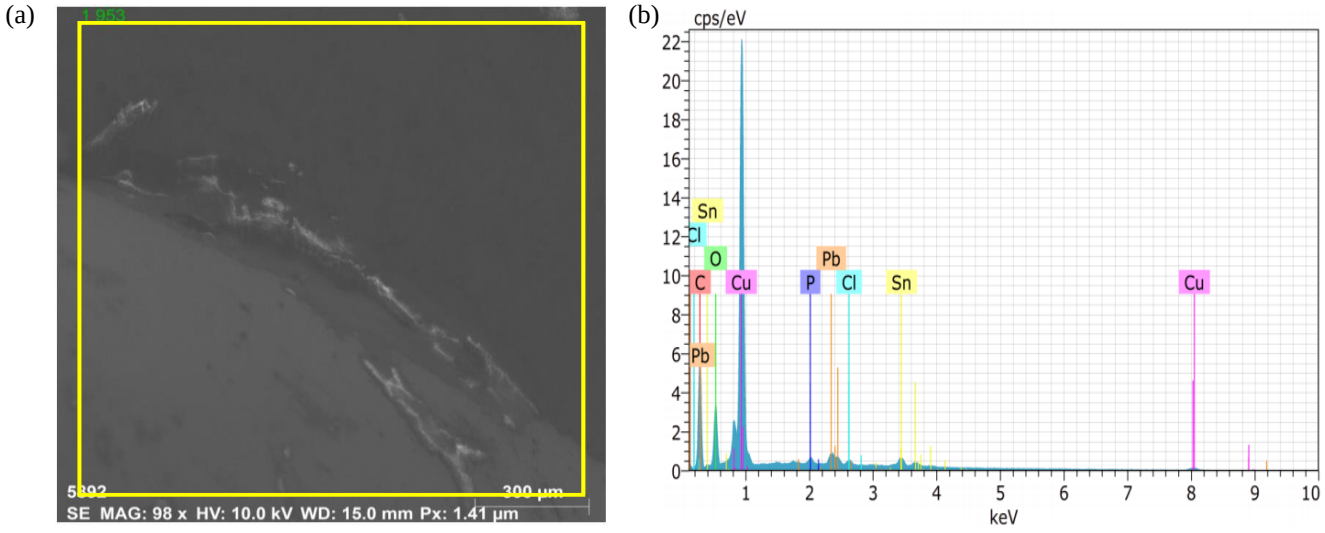

Figure 4. (a) SEM image of the sample showing the interface between copper and the solder (b) Energy Dispersive Spectroscopic analysis of different elements present in the sample.

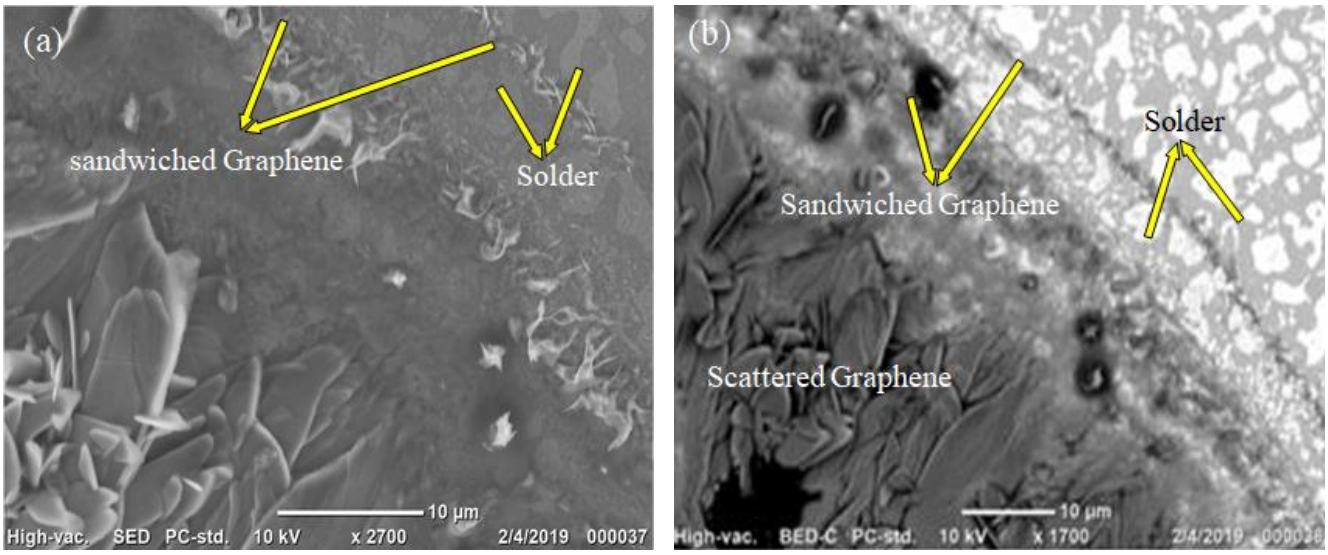

Figure 5. (a) Secondary electron detector (SED) image of graphene flakes and the solder (b) Backscattered electron detector (BED) image of graphene flakes and solder.

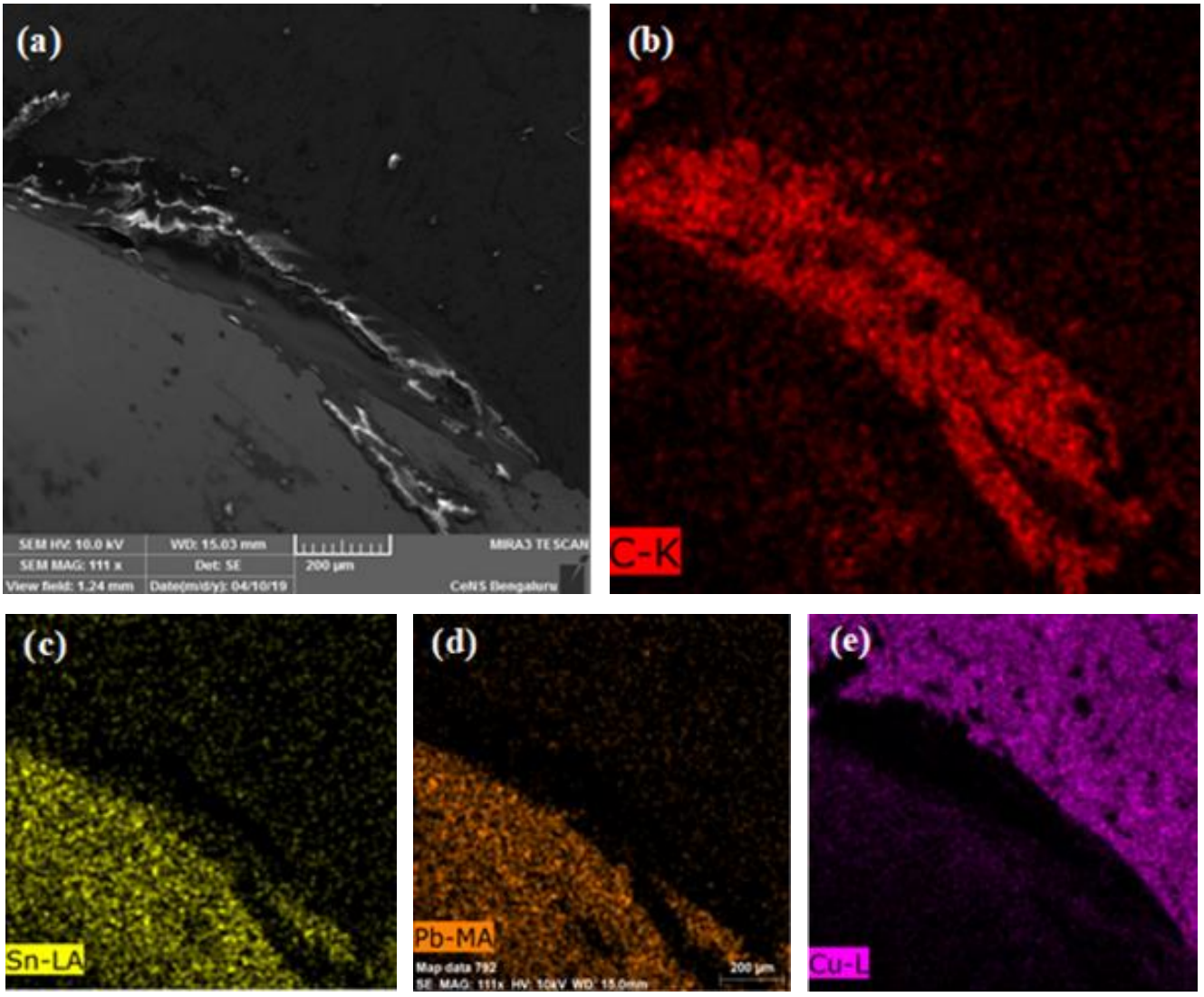

Figure 6. (a) SEM image of the sample showing the interface of copper, graphene, and solder (b) mapping of carbon (c) mapping of tin (d) mapping of lead and (e) mapping of copper.

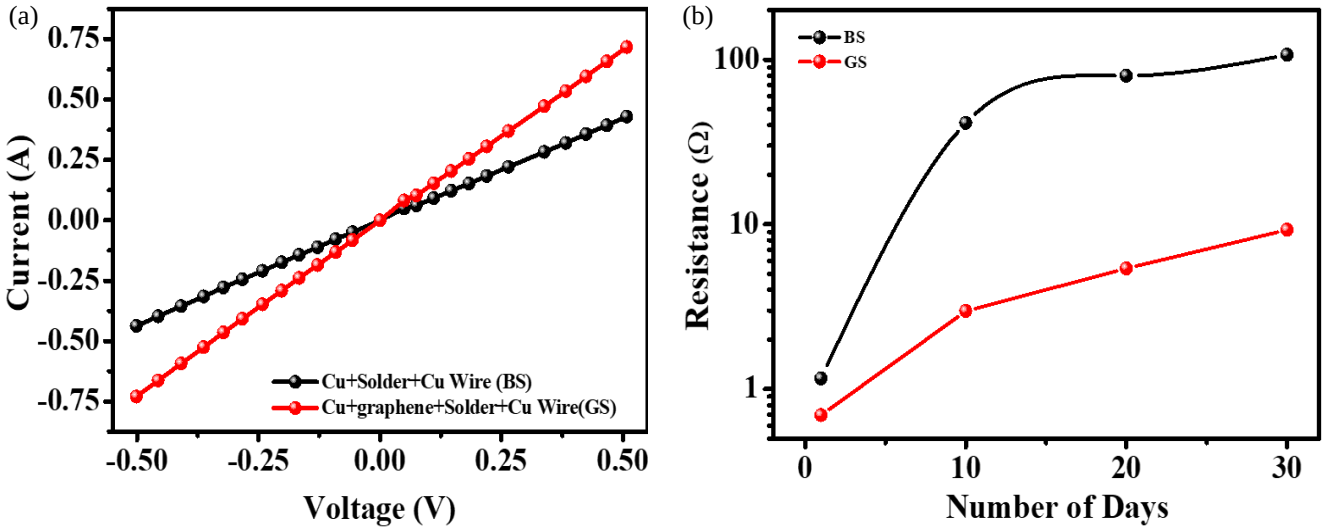

Figure 7.(a) Current-voltage characteristic of BS and GS (b) Logarithmic resistance vs. a number of days curves for BS and GS.

independently, as shown in Figure 6(c) and Figure 6(d) with yellow and orange color, respectively. As the process is carried out on the Cu substrate, the mapping is done for the Cu and shown in Figure 6(e) with a violet color. The elemental mapping of the sample confirms the presence of graphene between the interface. In the present work, graphene is used as an active material in the soldering process, graphene hinders the formation of intermetallics in between the solder and PCB. Copper do not wet graphene (graphene being hydrophobic in nature) and formation of covalent bond is not possible as no chemical reaction takes place between graphene and copper at temperatures around 260°C. Graphene is interfacially bond to Cu with adhesion energy that depends on the number of carbon layers in graphene and presence of structural defects in graphene which is confirmed by Raman analysis.

Finally, to understand the contact resistance, current-voltage characteristics is carried out for the interfaces of Cu > solder > Cu wire (bare soldering) (BS)and Cu > graphene > solder > Cu wire (graphene soldering) (GS) and it is shown in Figure 7(a). The calculated resistance values from the current-voltage curve are 1.16 and 0.69 Ω respectively for BS and GS. The surface oxidation of Cu hinders the diffusion of electrons, results in rise of resistance in BS. On the other side, graphene provides better diffusion of electrons, resulting less resistance in GS. Resistance is studied for a month in lab condition without any surface coatings which usually prevents oxidation in the commercial circuit boards, and it is shown in Figure 7(b). In the early ten days of duration, GS showed 2.28 Ω increment in the resistance and the BS showed increase in resistance of 40.0 Ω which indicates the oxidation of Cu in the PCB enhancing resistance at the interface. After 20 days of duration, GS and BS showed 5.39 and 79.60 Ω resistance respectively, which in turn indicates the Cu in the BS is rapidly getting oxidized resulting in the high resistance whereas GS also shows the small increment in the resistance due to the surface oxidation of Cu. Similarly, for a duration of 30 days the resistance of GS and BS were observed to be 9.26 and 106.73 Ω respectively. Though the resistance values are small, they affect any circuit and can produce thermal energy. Due to this resistance, the components in the circuit experience thermal energy. Hence the cooling system like fan and heat sinks used to dissipate the heat energy, which in turn results the extra load in the final product. Therefore, it is necessary to have less resistance in the interface of active component and solder.

The performance of the soldering joints is always understood in terms of their mechanical characteristics, such as tensile properties. Figure 8 shows the trend graph of load (N) versus extension (mm) for BS and GS. It can be seen that load is directly proportional to the extension until fracture. From the graph, two curves (black and red color) are not smooth and represent the slopes of 26.33 (BS) and 20.13 (GS) respectively. However, the represented curves are shown as loading progresses until failure. In case of BS, the solder is detached from the PCB at 700 N confirming the weak binding of solder on PCB, whereas in GS the Cu wire experienced lateral strain and it is fractured at 800 N, solder is intact with the PCB confirming higher strength.

The present method is economical, facile and can be incorporated in the commercial soldering processes in the industries. The developed graphene-based flux can prevent the resistive thermal energy at the interface and helps to avoid heat sinks and cooling fans to reduce the extra load in the final products.

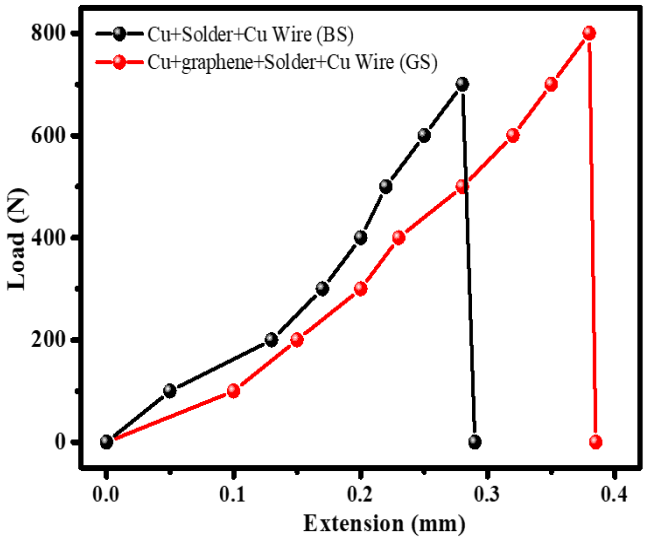

Figure 8. Graph of Load (N) versus Extension (mm).

4. Conclusions

A low-cost and durable graphene-based soldering flux is developed to enhance the soldering process. The prepared soldering flux showed high electrical conductivity and high stability. The presence of oxide layers on the bare Cu hinders the electrical conductivity. Therefore, graphene and ortho-phosphoric acid-based flux helps in eliminating the functional groups which ensures the better electrical conductivity. The performance of the developed soldering flux is understood by various characterizations and it is found to be superior over the conventional fluxes. Graphene can be synthesized easily, and the process is scalable and affordable. Hence, it can be implemented for industrial applications.

Acknowledgements

We thank Prof. G. U. Kulkarni, Director, CeNS, Bengaluru for his constant encouragement and support. We thank the Director, CEO, and Principal, Siddaganga Institute of Technology, Tumakuru, for continuous support and motivation. GP thanks Mr. Rajshekhar Pujar, Research Scholar, Centre for Nano and Soft Matter Sciences, Jalahalli, Bengaluru for the motivation. SM acknowledges the funding received from VGST, Govt of Karnataka. (VGST/GRD-585/2016-17/2017-18/39). AS and NM thanks to Karnataka Council for Technological Upgradation, Govt of Karnataka. (KCTU/R&D/SIT-Nano/2016- 17/399).

Supplementary data

Supplementary data to this article can be found online at https://doi.org/10.14456/jmmm.2020.xx.

References

[1] Q. Cao, H. Zhao, L. Xu, B. Lu, B. Wang, and Z. Song, "Effects of graphene nanosheets on the intermetallic compounds layer between Sn-Ag-Cu lead-free solders and Cu substrates," *IEEE Xplore*, pp. 1-3, 2015, https://ieeexplore.ieee.org/document/7411725.

[2] R. Mayappan, A. Saaleh, and J. Andas, "The effect of graphene on the intermetallic and joint strength of Sn-3.5Ag lead-free solder," *AIP Conference Proceedings*, vol. 1877, pp. 050004 1-8, 2017, https://doi.org/10.1063/1.4999878.

[3] J. Pstrus, P. Ozga, T. Gancarz, and K. Berent, "Effect of graphene layers on phenomena occurring at interface of Sn-Zn-Cu solder and Cu substrate," *Journal of Electronic Materials*, vol. 46, pp. 5248 1-11, 2017, https://doi.org/ 10.1007/s11664-017-5529-2.

[4] R.W. Wu, L.C. Tsao, and R.S. Chen, "Effect of 0.5 wt% nano-TiO_2 addition into low-$AgSn_{0.3}Ag_{0.7}$ Cu solder on the intermetallic growth with Cu substrate during isothermal aging," *Journal of Materials Science: Materials in Electronics*, vol. 26, pp. 1858-1865, 2015, https://doi.org/10.1007/ s10854-014-2621-8.

[5] I.M. Katsnelson, "Graphene: Carbon in two dimensions," *Materials Today*, vol. 10, pp. 20-27, 2007, https://doi.org/10.1016/S1369-7021(06)71788-6.

[6] H. Chen, M.B. Müller, K.J. Gilmore, G.G. Wallace, and D. Li, "Mechanically strong, electrically conductive, and biocompatible graphene paper," *Advanced Materials*, vol. 20, pp. 3557-3561, 2008, https://doi.org/10.1002/adma.200800757.

[7] Y. Zhu, S. Murali, W. Cai, X. Li, J.W. Suk, J.R. Potts, and R.S. Ruoff, "Graphene and graphene oxide: synthesis, properties, and applications," *Advanced Materials*, vol. 22, pp. 3906-3924, 2010, https://doi.org/10.1002/adma.201001068.

[8] J.C. Meyer, A.K. Geim, M.I. Katsnelson, K.S. Novoselov, T.J. Booth, and S. Roth, "The structure of suspended graphene sheets," *Nature*, vol. 446, pp. 60-63, 2007, https://doi:10.1038/nature05545.

[9] T.J. Booth, P. Blake, R.R. Nair, D. Jiang, E.W. Hill, U. Bangert, and A.K. Geim, "Macroscopic graphene membranes and their extraordinary stiffness," *Nano Letters*, vol. 8, pp. 2442-2446, 2008, https://doi.org/10.1021/nl801412y.

[10] S.Y. Yang, K.H. Chang, Y.L. Huang, Y.F. Lee, H.W. Tien, S.M. Li, and C.C. Hu, "A powerful approach to fabricate nitrogen-doped graphene sheets with high specific surface area," *Electrochemistry Communications*, vol. 14, pp. 39-42, 2012, https://doi.org/10.1016/ j.elecom.2011.10.028.

[11] I.S. Burmistrov, I.V. Gornyi, V.Y. Kachorovskii, M.I. Katsnelson, and A.D. Mirlin, "Quantum elasticity of graphene: Thermal expansion coefficient and specific heat," *Physical Review B*, vol. 94, pp. 1-18, 2016, https://doi.org/10.1103/PhysRevB.94.195430.

[12] D.A.C. Brownson, and C.E Banks, "Graphene electrochemistry: An overview of potential applications," *The Analyst*, vol. 135, pp. 2768-2778, 2010, https://doi.org/10.1039/C0AN00590H.

[13] T. Kuila, S. Bose, A.K. Mishra, P. Khanra, N.H. Kim, and J.H. Lee, "Chemical functionalization of graphene and its applications," *Progress in Materials Science*, vol. 57, pp. 1061-1105, 2012, https://doi.org/10.1016/j.pmatsci.2012.03.002.

[14] D.C. Marcano, D.V. Kosynkin, J.M. Berlin, A. Sinitskii, Z. Sun, A. Slesarev, and J.M. Tour, "Improved Synthesis of Graphene Oxide," *ACS Nano*, vol. 4, pp. 4806-4814, 2008, https://doi.org/ 10.1021/nn1006368.

[15] A.N. Obraztsov, "Making graphene on a large scale," *Nature Nano-technology*, vol. 4, pp. 212-213, 2009, https://doi:10.1038/nnano.2009.67.

[16] S. Stankovich, D.A. Dikin, R.D. Piner, K.A. Kohlhaas, A. Kleinhammes, Y. Jia, and R.S. Ruoff, "Synthesis of graphene-based nanosheets via chemical reduction of exfoliated graphite oxide," *Carbon*, vol. 45, pp. 1558-1565, 2007, https://doi.org/ 10.1016/j.carbon.2007.02.034.

[17] C.Y. Su, A.Y. Lu, Y. Xu, F.R. Chen, A.N. Khlobystov, and L.J. Li, "High-quality thin graphene films from fast electrochemical exfoliation," *ACS Nano*, vol. 5, pp. 2332-2339, 2011, https://doi.org/10.1021/nn200025p.

[18] S. Mundinamani, "The choice of noble electrolyte for symmetric polyurethane-graphene composite supercapacitors," *International Journal of Hydrogen Energy*, vol. 44, pp. 11240-11246, 2019, https://doi.org/10.1016/j.ijhydene.2019.02.164.

[19] W. Jang, Z. Chen, W. Bao, C.N. Lau, and C. Dames, "Thickness-dependent thermal conductivity of encased graphene and ultrathin graphite," *Nano Letters*, vol. 10, pp. 3909-3913, 2010, https://doi.org/10.1021/nl101613u.

[20] W. Gao, L.B. Alemany, L. Ci, and P.M. Ajayan, "New insights into the structure and reduction of graphite oxide," *Nature Chemistry*, vol. 1, pp. 403-408, 2009, https://doi:10.1038/ nchem.281.

[21] T.J. Fatima, W.L. Jee, and G.J. Woo, "Facile and safe graphene preparation on solution based platform," *Journal of Industrial and Engineering Chemistry*, vol. 20, pp. 2883-2887, 2014, https://doi.org/10.1016/j.jiec.2013.11.022.

[22] I.K. Moon, J. Lee, R.S. Ruoff, and H. Lee, "Reduced graphene oxide by chemical graphitization," *Nature Communications*, vol. 1, pp. 1-6, 2010, https://doi:10.1038/ ncomms1067.

[23] B.W. Jiang, L.L. Miao, C. Xin, N.L. He, and H.T. Ping, "Raman spectroscopy of graphene-based materials and its applications in related devices," *Chemical Society Reviews*, vol. 47, pp. 1822-1873, 2018, https://doi.org/10.1039/C6CS00915H.

[24] K.N. Konstantin, O. Bulent, C.S. Hannes, K.P. Robert, A.A. Ilhan, and C. Roberto, "Raman spectra of graphite oxide and functionalized graphene sheets," *Nano Letters*, vol. 8, pp. 36-41, 2008, https://doi.org/10.1021/nl071822y.

[25] J.A. Small, "The analysis of particles at low accelerating voltages (10 kV) with energy dispersive x-ray spectroscopy (EDS)," *Journal of Research of the National Institute of Standards and Technology*, vol. 107, pp. 555-556, 2002, https://doi.org/10.6028/jres.107.047.